Am. J. Hum. Genet. 64:1158–1165, 1999

Relaxed Replication of mtDNA: A Model with Implications for the Expression of Disease

Patrick F. Chinnery[1] and David C. Samuels[2]

Departments of [1]Neurology and [2]Mathematics, The University of Newcastle upon Tyne, Newcastle upon Tyne, United Kingdom

Summary

Heteroplasmic mtDNA defects are an important cause of human disease with clinical features that primarily involve nondividing (postmitotic) tissues. Within single cells the percentage level of mutated mtDNA must exceed a critical threshold level before the genetic defect is expressed. Although the level of mutated mtDNA may alter over time, the mechanism behind the change is not understood. It currently is not possible to directly measure the level of mutant mtDNA within living cells. We therefore developed a mathematical model of human mtDNA replication, based on a solid foundation of experimentally derived parameters, and studied the dynamics of intracellular heteroplasmy in postmitotic cells. Our simulations show that the level of intracellular heteroplasmy can vary greatly over a short period of time and that a high copy number of mtDNA molecules delays the time to fixation of an allele. We made the assumption that the optimal state for a cell is to contain 100% wild-type molecules. For cells that contain pathogenic mutations, the nonselective proliferation of mutant *and* wild-type mtDNA molecules further delays the fixation of both alleles, but this leads to a rapid increase in the mean percentage level of mutant mtDNA within a tissue. On its own, this mechanism will lead to the appearance of a critical threshold level of mutant mtDNA that must be exceeded before a cell expresses a biochemical defect. The hypothesis that we present is in accordance with the available data and may explain the late presentation and insidious progression of mtDNA diseases.

Received June 9, 1998; accepted for publication January 21, 1999; electronically published March 2, 1999.

Address for correspondence and reprints: Dr. Patrick F. Chinnery, Department of Neurology, The University of Newcastle upon Tyne, The Medical School, Framlington Place, Newcastle upon Tyne, NE2 4HH, United Kingdom. E-mail: P.F.Chinnery@ncl.ac.uk

0002-9297/99/6404-0030$02.00

Introduction

mtDNA defects cause a diverse group of diseases that often result in severe morbidity and premature death (Wallace 1992; Johns 1995; Shoffner 1996). Individuals with pathogenic mtDNA defects (deletions and point mutations) usually harbor a mixture of mutant and wild-type mtDNA within each cell (heteroplasmy; Larsson and Clayton 1995). In vitro studies have shown that the percentage level of mutant mtDNA must exceed a critical threshold level before a cell expresses a mitochondrial respiratory-chain deficiency (Attardi et al. 1995). The percentage level of heteroplasmy varies between different organs and also between adjacent cells within the same organ. These differences are partly due to the differential partitioning of mitochondrial genomes, between daughter cells, during embryological development (vegetative segregation; Lightowlers et al. 1997). However, there is increasing evidence that the level of mutant mtDNA in nondividing (postmitotic) tissues may change during a human lifetime (Larsson et al. 1990; Poulton and Morten 1993; Weber et al. 1997). The most disabling manifestations of mtDNA disease arise through the clinical involvement of postmitotic tissues such as skeletal muscle and neurons (Chinnery and Turnbull 1997), and changes in mutation load, with advancing age (longitudinal changes), may explain the late presentation and insidious progression of mtDNA diseases (Wallace 1995). Our understanding of mitochondrial disease, therefore, is critically dependent on our knowledge of the mechanisms that determine the level of mutant mtDNA within the cell, but, in the foreseeable future, it is unlikely that we will be able to measure this level directly. We therefore chose a mathematical approach to the investigation of the potential longitudinal changes in mtDNA heteroplasmy in human cells.

Each mammalian mitochondrion contains 2–10 copies of mtDNA, resulting in 1,000–100,000 copies in each human cell (Larsson and Clayton 1995; Lightowlers et al. 1997). Despite the high copy number, recombination of mtDNA molecules is rare (Howell 1997), and each mtDNA molecule replicates independently. Nuclear DNA replicates once during the cell cycle. By contrast, mtDNA turns over continuously. Individual mtDNA

molecules replicate at random, making one or more copies at a time while maintaining a relatively constant total number of mtDNA molecules within the cell (relaxed replication; Birky 1994). If there are two or more different types of mtDNA molecules within a cell, then, by chance, any one type of molecule may replicate more frequently than another type, resulting in a change in the level of heteroplasmy within the cell (intracellular drift).

We developed a computer simulation of a somatic human cell containing a mixed, nonpartitioned (panmictic) population of two different mtDNA molecules. Because the model was developed to increase our understanding of mtDNA disease, our simulations always began with >1% mutant mtDNA within the cell, and we assumed that rare somatic mutations had no significant effects. We based the model on experimentally derived parameters. Any inaccuracies in these parameters may have influenced the absolute values predicted, but they are unlikely to have altered the overall trends. We first studied the dynamics of intracellular heteroplasmy for two neutral alleles and then studied the effects of a pathogenic allele.

The Basic Model: Two Neutral Alleles

We assumed that, in a collection of mtDNA molecules containing two distinct neutral alleles, A and B, each molecule was destroyed with a half-life, $T_{1/2}$, of 1–10 d (Gross et al. 1969). If new mtDNA molecules are generated at a copy rate C, then the total number N of mtDNA molecules within each simulated cell changes at the following rate:

$$\frac{dN}{dt} = C - \frac{N}{\tau}\ , \qquad (1)$$

where $\tau = T_{1/2}/\ln(2)$. If the bioenergetic demands on the cell remain constant, the cells harboring neutral mitochondrial alleles are likely to maintain a relatively stable number of mtDNA molecules (Clayton 1996). We called this value "N_{Optimal}." In order to maintain a steady number of mtDNA at N_{Optimal}, the copy rate, determined from equation (1), must be $C = N_{\text{Optimal}}/\tau$. Starting with an initial population of mtDNA molecules within a single cell, each mtDNA molecule has a probability $\Delta t/\tau$ of being destroyed during a given time step Δt. Destroyed mtDNA molecules were removed from the population. We then calculated the number of new mtDNA molecules, $N_{\text{New}} = C\Delta t$, that were created during the same time step and made a single copy of N_{New} randomly chosen molecules from the remaining population. This process was repeated for each time increment. Although an mtDNA molecule may be copied more than once when it replicates (Birky 1994), this is unusual in mammalian cells (Flory and Vinograd 1973). For simplicity, we report here the results for single replications.

Figure 1*a* and *b* shows the results of 10 independent and representative simulation runs for single cells. Each cell contains ~1,000 mtDNA molecules in which the initial proportions of the two alleles were 75% for allele A and 25% for allele B. Simulated cells that began with the same initial proportions of alleles A and B developed radically different mtDNA populations over a short period of time, and the level of heteroplasmy within any one cell varied greatly throughout the simulation. The average proportions of the two neutral alleles, for as few as 10 simulated cells, remained relatively constant (approximately equal to the starting values). This suggests

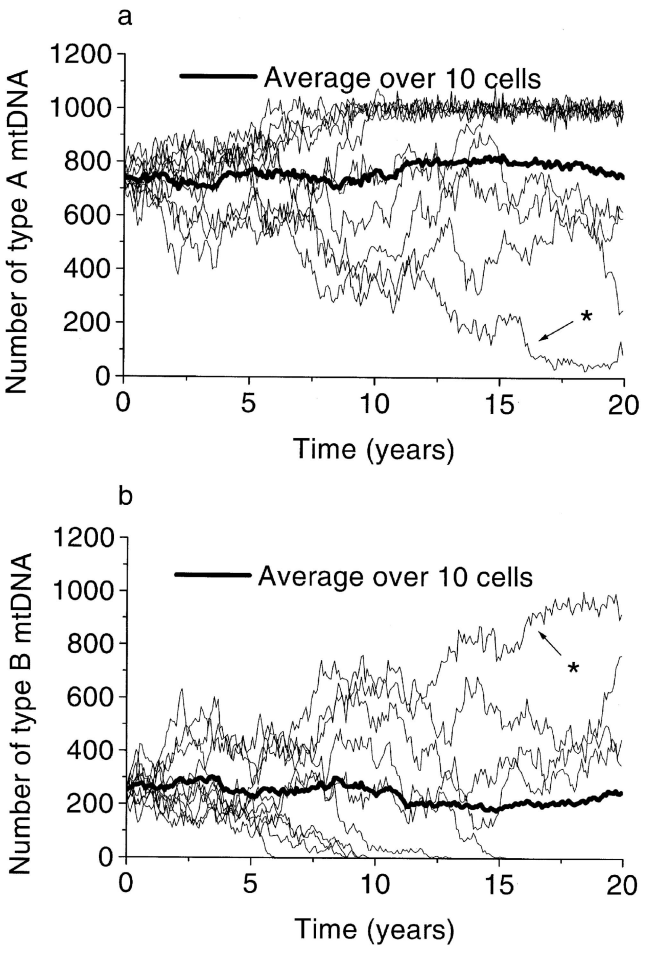

Figure 1 Number of molecules of neutral allele A (*a*) and neutral allele B (*b*), for 10 independently simulated cells. Each simulated cell started with proportions of 75% for allele A and 25% for allele B and with 1,000 mtDNA molecules. Each cell trace in panel *a* has a corresponding trace in panel *b* (e.g., see the traces marked by an asterisk [*]). The mean numbers of alleles A and B, averaged over the 10 cells, are shown by the boldface line. Over a short period of time, the frequency of each allele varied markedly, and there was a striking difference between any two simulated cells.

that *single* measurements of heteroplasmy in small tissue homogenates or in single cells may be of limited value in elucidating the cellular mechanisms underlying a longitudinal change. However, by use of this model, insight into these processes should be possible, by the study of the *distribution* of heteroplasmy in a large number of individual cells, at two or more points in time.

We then studied the probability of fixation for a particular allele, by performing sufficient simulation runs to ensure that ~1,000 cells became fixed on that allele. Statistical measurements then were made on the subpopulation of cells that eventually fixed on the chosen allele. We then constructed the probability distribution curves for the fixation time for each allele, over a range of different values for the initial proportions of allele A and allele B, for cells containing 100–2,000 mtDNA molecules and for a $T_{1/2}$ of 1–10 d. We tested the probability distributions generated by the simulations against a large number of known probability distributions. The inverse Gaussian (Wald) distribution accurately described the distribution drawn from our simulation data (fig. 2*a;* Johnson et al. 1995). This may be written as a function of the probability density $p(t)$ of fixation at time t:

$$p(t) = \sqrt{\frac{\lambda}{2\pi t^3}}\ \exp\left[\frac{-\lambda}{2\mu^2 t}(t-\mu)^2\right] , \qquad (2)$$

where μ is the mean time to fixation and λ is a parameter that determines the shape of the distribution. By measuring this probability distribution for many different values of the simulation parameters, we found that the quantities μ and λ were simple functions of the initial allele frequency N_{Optimal} and of $T_{1/2}$ (fig. 2*b* and *c*). By use of figure 2*b* and *c,* the mean time to fixation for any initial population of mtDNA molecules can be determined, given the average number of mtDNA molecules in the cell (N_{Optimal}) and the half-life ($T_{1/2}$).

We made four important observations. First, the distribution was highly skewed, with a long positive tail: the final 25% of the cells took much longer to fix than the first 25% of the cells. Second, the mean time to fixation was proportional to the number of mtDNA molecules within the simulated cell and was a function of the initial allele frequency (fig. 2*b*). Third, shortening of the mtDNA half-life proportionately shortened the mean time to fixation (fig. 2*b*). Finally, the proportion of cells that became fixed for any particular allele was equal to the initial allele frequency, as would be expected for any simple model of random intracellular drift.

The Disease Model: Wild-Type and Pathogenic Alleles

In a healthy cell, the number of mtDNA molecules is tightly regulated (Turnbull and Lightowlers 1998). By contrast, mtDNA proliferation is one of the hallmarks of heteroplasmic mtDNA mutations involving tRNA genes (rearrangements and point mutations) (Mita et al. 1989; Shoubridge et al. 1990; Moraes et al. 1992; Tokunaga et al. 1994). In skeletal muscle fibers, these mutations are accompanied by mitochondrial proliferation in the subsarcolemal space (giving rise to a so-called ragged-red appearance). mtDNA proliferation also occurs in other tissues (Kaufmann et al. 1996), which suggests that it is an essential compensatory response to the presence of a pathogenic allele (Schon et al. 1997). In developing the disease model, we therefore made the assumption that the optimal state for a cell was to contain the same number of wild-type molecules as a cell that did not contain any mutant mtDNA. As in the basic model, we called this number "N_{Optimal}." If a cell did not contain N_{Optimal} wild-type molecules, then the *total* intracellular mtDNA pool would proliferate in an attempt to redress the balance.

Although it is likely that any one pathogenic mutation would result in only a relative deficiency of mtDNA expression (Schon et al. 1997), we assumed, for simplicity, that the pathogenic allele rendered the mitochondrial gene completely functionless. Pathological mtDNA proliferation was incorporated into the model by identification of our two types of mtDNA as "wild-type" and "mutant." We then made the mtDNA population copy rate C a linear function of the number of wild-type mtDNA, N_{Wild}, according to the following equation: $C = C_0[\alpha + (1-\alpha)(N_{\text{Wild}}/N_{\text{Optimal}})]$, where $C_0 = N_{\text{Optimal}}/\tau$ and where the growth coefficient α is a constant >1. Thus, when the cell contains the optimal number of wild-type mtDNA (i.e., when $N_{\text{Wild}} = N_{\text{Optimal}}$), the copy rate is $C = C_0$, which is identical to that for neutral alleles (see eq. [1]). As the number of wild-type mtDNA molecules falls below N_{Optimal}, the copy rate increases linearly until it reaches a maximum value of αC_0 when $N_{\text{Wild}} = 0$. Increasing the copy rate by a factor of α causes the stable number of mtDNA to increase by the same factor α. We derived α from experimentally determined values for maximal mtDNA proliferation (5–17-fold [Mita et al. 1989; Shoubridge et al. 1990; Moraes et al. 1992; Tokunaga et al. 1994]). Thus, in this model, the mutant mtDNA molecule *does not* have a replicative advantage over a wild-type molecule. The other parameters of the basic simulation were left unchanged.

Figure 3*a* and *b* shows a typical time evolution for the wild-type and mutant alleles in 10 individual simulations. The development of the two populations was strikingly different. Within an individual cell, the number of wild-type alleles tended to remain close to the optimal value, whereas the number of mutant alleles fluctuated greatly. As with the simple model, the total number of cells that became fixed on each allele was

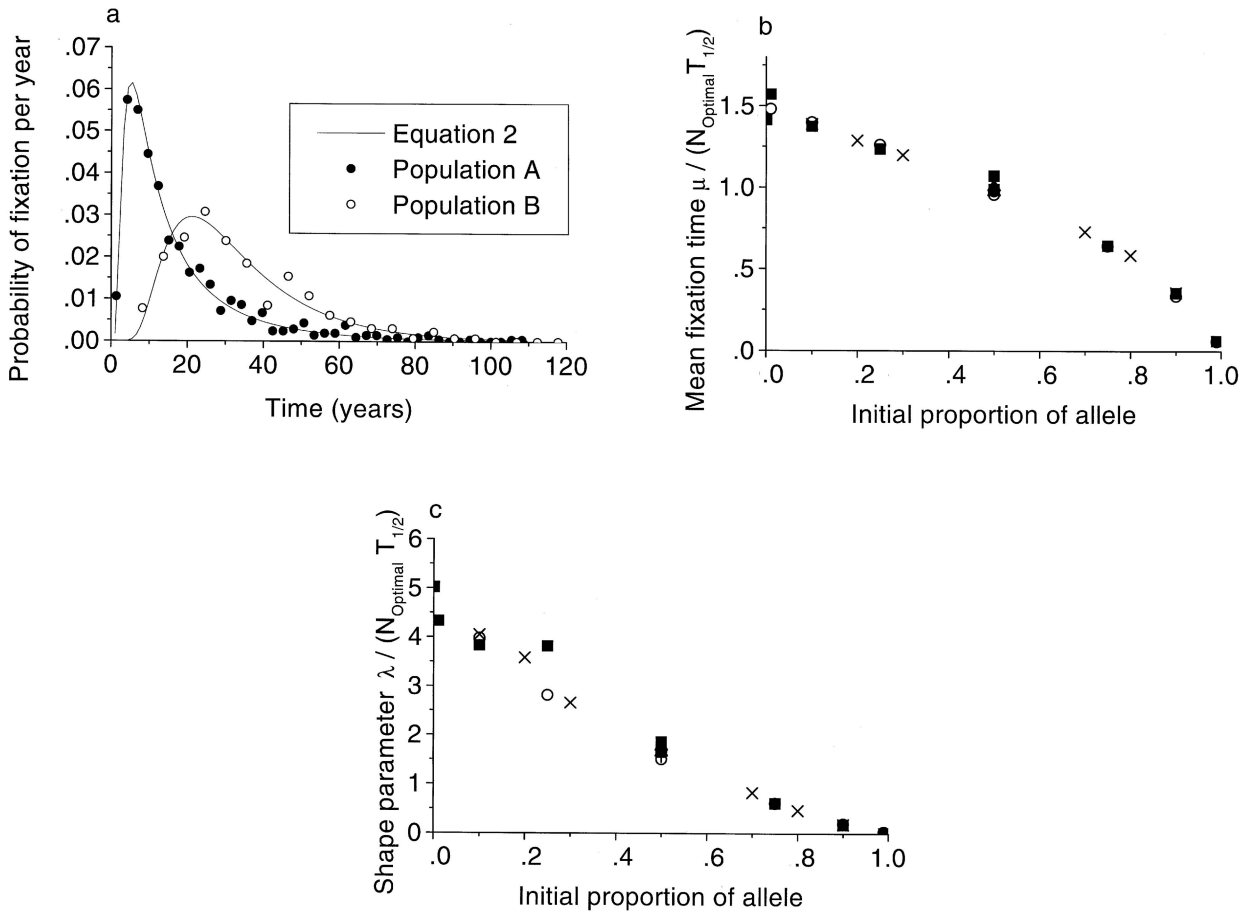

Figure 2 *a,* Probability density of fixation of the alleles, for the simulations in figure 1. The data points are the values calculated from the simulations, and the curves show the inverse Gaussian (Wald) distribution (eq. [2]). These probability distributions have long positive tails. *b,* Relationship between mean time to fixation and initial allele frequency p for the simulated cells. Each data point was calculated from 1,000–100,000 cell simulations with different basic parameters: an unblackened circle indicates $N_{Optimal} = 100$ and $T_{1/2} = 10$ d; a blackened triangle indicates $N_{Optimal} = 200$ and $T_{1/2} = 10$ d; a blackened square indicates $N_{Optimal} = 1{,}000$ and $T_{1/2} = 10$ d; a plus sign (+) indicates $N_{Optimal} = 2{,}000$ and $T_{1/2} = 10$ d; and a multiplication sign (×) indicates $N_{Optimal} = 100$ and $T_{1/2} = 1$ d. The mean time to fixation is a function of the initial allele proportion and is proportional to $T_{1/2}$ and the number of mtDNA molecules within a cell. When the curve is extrapolated to an initial $p \approx 0$, 50% of the cells that eventually become fixed on this allele will become fixed within a time $t \approx 1.5\ (NT_{1/2})$. As p approaches 0, the fraction of cells that fix on this allele also approaches 0. *c,* Probability distribution–shape parameter λ as a function of the initial population, the number of mtDNA molecules, and $T_{1/2}$. This curve can be used to calculate the probability distribution (*panel a*) of the fixation times, determined by equation (2), for a given mean fixation time μ (symbols defined as for *panel b*).

equal to the initial starting frequency for that allele. However, the mean time to fixation in these simulations was delayed for both the wild-type and mutant alleles (fig. 4). This delay was greater for cells that ultimately became fixed on the mutant allele, and, as a consequence, the time that each cell maintained a near-optimal number of wild-type mtDNA molecules was greatly lengthened.

We also observed an inverse correlation between the levels of the mutant and wild-type alleles. Over a large number of independent simulations, the level of mutant mtDNA was found to be related to the level of wild-type mtDNA, according to the following equation:

$$N_{Wild} + \frac{1}{\alpha} N_{Mutant} \approx N_{Optimal} \ . \qquad (3)$$

If $R_{Mutant} = N_{Mutant}/N_{Total}$ (the percentage mutation load, a value that usually is determined for patients with mtDNA disease) and $N_{Total} = N_{Wild} + N_{Mutant}$, then equation (3) can be written in terms of $N_{Wild}/N_{Optimal}$:

$$\frac{N_{Wild}}{N_{Optimal}} = \frac{\alpha(1 - R_{Mutant})}{\alpha + (1 - \alpha)R_{Mutant}} \ . \qquad (4)$$

Figure 5 shows a plot of equation 4. When $\alpha = 1$ (as in

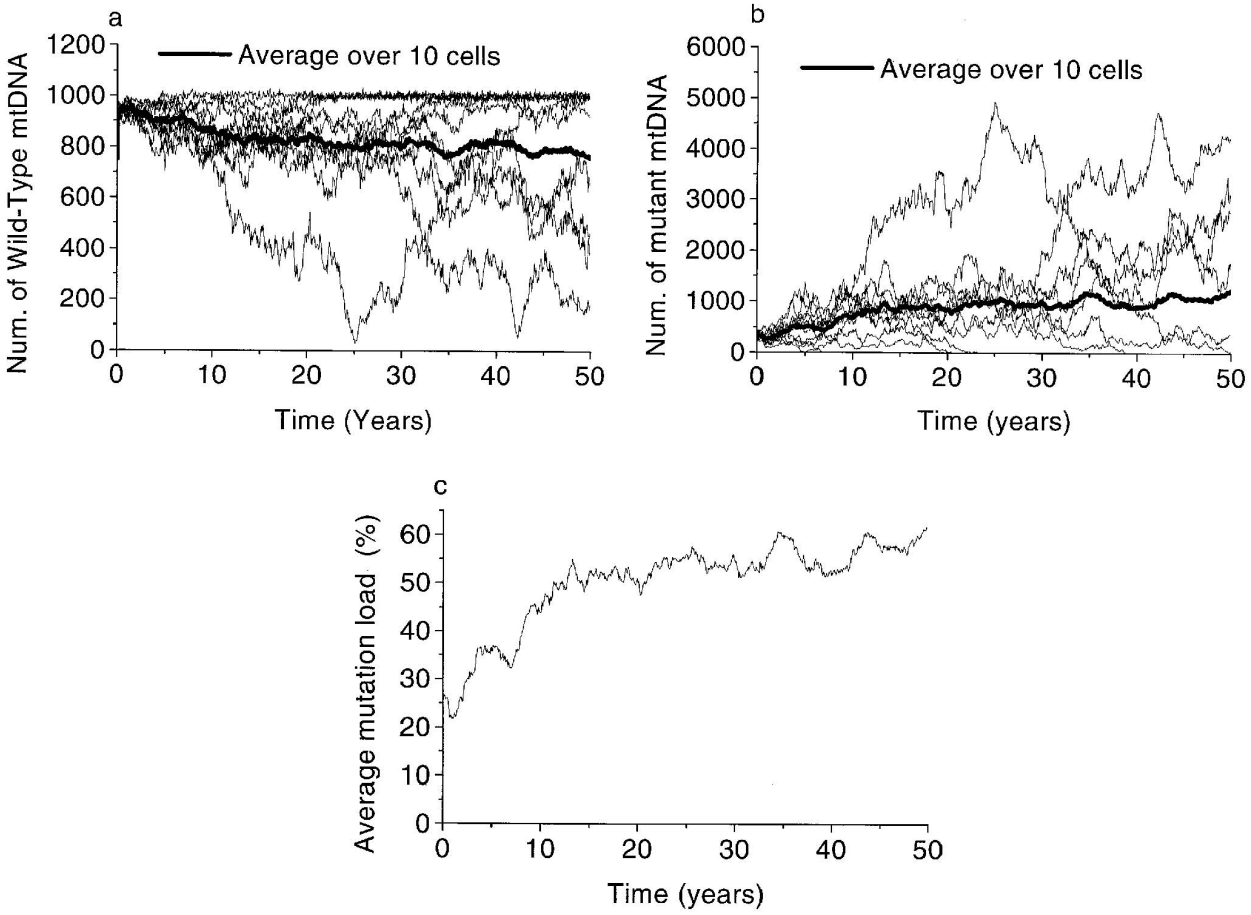

Figure 3 Number of molecules of wild-type allele (*a*) and mutant allele (*b*) in the disease model. Results for 10 independently simulated cells are shown, and each cell initially contained 1,000 mtDNA molecules with 75% wild-type and 25% mutant mtDNA. In these simulations the mtDNA population in individual cells increased up to fivefold ($\alpha = 5$) in response to the number of wild-type mtDNA molecules within the simulated cell (see text). The mean numbers of mutant and wild-type alleles, averaged over the 10 cells, are shown by the boldface lines (*panels a* and *b*). The mean percentage of mutant mtDNA (*panel c*), averaged over the 10 cells, showed a progressive increase with time.

the basic model), the relationship $N_{\text{Wild}}/N_{\text{Optimal}}$ against $N_{\text{Mutant}}/N_{\text{Total}}$ was linear. However, with increasing values of α, a "shoulder" appeared in the graph. For cells containing low to moderate levels of mutant mtDNA, the ratio $N_{\text{Wild}}/N_{\text{Optimal}}$ remained approximately constant and near unity. In other words, the cell maintained a level of wild-type mtDNA that was similar to the level in cells that contained no mutant mtDNA (homoplasmic wild-type mtDNA). However, once a critical level of mutant mtDNA was exceeded, then the ratio $N_{\text{Wild}}/N_{\text{Optimal}}$ fell abruptly.

Because an individual cell maintained a near-optimal level of wild-type mtDNA at the expense of an increasing level of mutant mtDNA, the mean percentage level of mutant mtDNA, averaged over a number of cells, increased with time (fig. 3*c*). The mean value shown in figure 3*c* was obtained from an average over only 10 cells, and, even with this small number of cells, the large fluctuations seen in the individual cells were not apparent.

Discussion

Precisely how a cell fixes or removes a pathogenic mtDNA mutation is fundamentally important to our understanding of the relationship between the mitochondrial genome and disease. It seems intuitive that a high mtDNA copy number will protect against the accumulation of deleterious mutations, but how this protective effect might occur has not been clear. Our model has shown that, within the constraints of human physiology, relaxed replication *alone* will tend to prevent new mutations from reaching significant levels. If correct, it is highly unlikely that such a fundamentally important mechanism would have arisen by chance. Human mtDNA accumulates mutations at 10–16 × the rate of

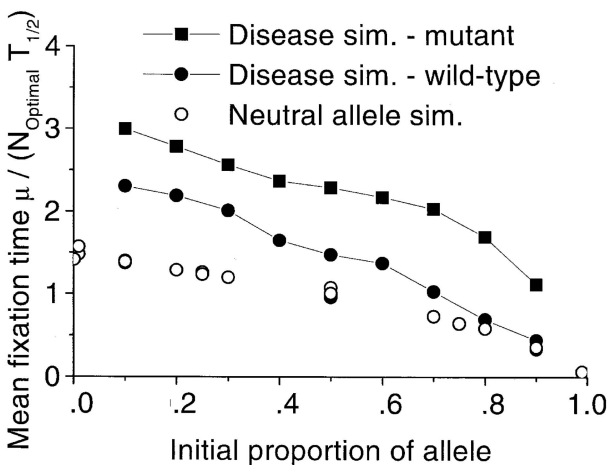

Figure 4 Relationship between mean time to fixation and initial allele frequency, for the disease model. Simulated cells initially contained 1,000 mtDNA molecules, and we set $\alpha = 5$ (see text). The unblackened circles indicate neutral alleles (as in fig. 1*b*). Proliferation delays the mean time to fixation, for both mutant and wild-type alleles. For cells that ultimately become fixed on mutant mtDNA, the delay is greater than for those that become fixed on wild-type mtDNA.

the nuclear genome (Larsson and Clayton 1995), but, despite the importance of each mitochondrial gene, mitochondria are relatively deficient in DNA-repair mechanisms (Lightowlers et al. 1997). The results that we present here are consistent with the hypothesis that, at least in part, human cells contain a high copy number of mtDNA molecules in order to protect them against the accumulation of mutant alleles during their lifetime. This may be part of the reason why short-lived human cells (such as leukocytes and sperm [Zhang et al. 1994; Ankel-Simons and Cummins 1996]) have a low mtDNA copy number ($\leq$1,000), despite a heavy dependence on mitochondrial oxidative metabolism, whereas long-lived cells (such as skeletal muscle cells, central neurons, and oocytes [Lightowlers et al. 1997]) contain many mtDNA molecules (>100,000).

This model also sheds light on the mechanisms that potentially are responsible for the late presentation and progression of mtDNA diseases. In designing the model, we assumed that each cell attempts to maintain an optimal level of native mtDNA and that each cell must "sense" that it does not contain an optimal number of wild-type molecules. This mechanism presumably is a function of the nucleus and does not necessarily need to occur through a biochemical respiratory-chain deficiency (Schon et al. 1997). The proliferation of mtDNA will delay the time necessary to fix an allele but only up to a critical point (fig. 5). After this point, relaxed replication will lead to an abrupt *reduction* in the number of wild-type molecules, which has two important consequences. First, the mean tissue level of mutant mtDNA will increase over time (fig. 3*c*). This increase occurs through the proliferation of mtDNA in heteroplasmic cells that contain suboptimal levels of wild-type mtDNA. Thus, this model illustrates a potential mechanism for the accumulation of mutant molecules in postmitotic tissues; it is supported by observations from the study of patients with progressive mtDNA disease (Larsson et al. 1990; Weber et al. 1997); and it may explain the late presentation and subsequent clinical progression in patients with mtDNA disease (Wallace et al. 1995). Second, on the basis of this model, measurements of single cells likely will fall into one of two groups. Those cells with percentage levels of mutant mtDNA *below* the abrupt shoulder will contain a near-normal number of wild-type mtDNA molecules. By contrast, cells with percentage levels of mutant mtDNA *above* the abrupt shoulder will contain substantially less wild-type mtDNA molecules. Thus, for cells around this transition zone, subtle changes in the percentage of mutant mtDNA will be accompanied by dramatic changes in the amount of wild-type mtDNA. This effect, on its own, will lead to the appearance of a critical threshold level of mutant mtDNA that must be exceeded before the genetic defect is expressed. This model suggests that the threshold effect (Wallace 1995) is a direct consequence of the maintenance of wild-type copy numbers by relaxed replication of mtDNA.

In patients with mtDNA disease, different genetic defects have subtly different effects on mtDNA expression

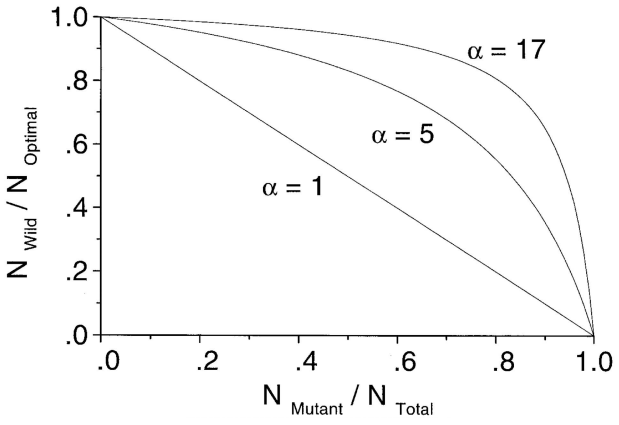

Figure 5 Relationship between number of wild-type mtDNA (N_{Wild}), relative to the optimal number ($N_{Optimal}$), against the percentage of mutant mtDNA (N_{Mutant}/N_{Total}), for different values of maximal proliferation α. Proliferation of mitochondrial genomes in a simulated disease cell maintains near-optimal levels of wild-type mtDNA, up to a critical point. Beyond this point, further proliferation results in a massive increase in mutant genomes, and the level of wild-type mtDNA rapidly falls below the optimal level. Higher maximal levels of proliferation (i.e., higher α values) maintain near-optimal levels of wild-type mtDNA for a longer period of time but result in a more abrupt transition from $N_{Wild} \approx N_{Optimal}$ to a predominance of mutant molecules.

(Moraes et al. 1992; Schon et al. 1997). In our disease model, α is related to the maximal rate of proliferation of mtDNA measured in vivo and, thus, reflects the nature of the genetic defect. A higher level of α not only will delay the time to fixation of an allele but also will determine the abruptness *and* the absolute level of the apparent critical threshold. Since mtDNA proliferation is a response to the presence of suboptimal mtDNA molecules, higher rates of mtDNA proliferation will occur in cells harboring molecules that have a major effect on mtDNA function. According to our model, this will lead to a high apparent threshold (80%–90% for $\alpha = 17$), which is consistent with observations from the study of patients with the A3243G MELAS (mitochondrial myopathy, encephalopathy, lactic acidosis, and stroke-like episodes) mutation (Tokunaga et al. 1994) and the A8344G MERRF (myoclonic epilepsy with ragged red fibers) mutation (Boulet et al. 1992). By contrast, mutations that have a less detrimental effect will be accompanied by less proliferation, and the apparent threshold will be less abrupt and at a lower value (50%–70% for $\alpha = 7$). This is consistent with observations from the study of patients harboring mtDNA deletions (Hayashi et al. 1991; Shoubridge 1994). The extreme variability both between and within our simulated cells highlights the need for many measurements when single cells are studied (figs. 1 and 3). This variability also may explain apparently conflicting data from different laboratories (Mita et al. 1989; Shoubridge et al. 1990; Moraes et al. 1992; Tokunaga et al. 1994).

We present this model as a hypothesis that is supported by experimental observation. The expression of mtDNA is complex, and we recognize that nuclear and mitochondrial genetic factors may influence the transcription and translation of mitochondrial genes (Larsson et al. 1998; Turnbull and Lightowlers 1998). This model is not intended to provide a comprehensive explanation of human mtDNA maintenance and expression. For example, we have not considered the possibility of more than two alleles within a cell, because significant levels of triplasmy are probably very rare (Lightowlers et al. 1997). Furthermore, the intracellular drift of mtDNA heteroplasmy likely will be influenced by the packaging of mtDNA into discrete units (such as mitochondria or nucleoids), which we will include in later models. We believe, however, that the simulations we have described clearly demonstrate the potential for temporal dynamics of intracellular heteroplasmy in human cells. Relaxed replication also may be involved in the clonal expansion of somatic mtDNA mutations during aging (Brierley et al. 1998) and may contribute to the diverse genotypes and phenotypes seen in families harboring pathogenic mtDNA mutations (Lightowlers et al. 1997), further highlighting the importance of this mechanism in our understanding of mtDNA and its relationship to aging and disease.

Acknowledgments

We are indebted to Prof. Neil Howell for his comments during the preparation of this manuscript and to Prof. Douglass Turnbull and Dr. Bob Lightowlers for their support. P.F.C. is a Wellcome Trust Research Fellow.

References

Ankel-Simons F, Cummins JM (1996) Misconceptions about mitochondria and mammalian fertilization: implications for theories on human evolution. Proc Natl Acad Sci USA 93: 13859–13863

Attardi G, Yoneda M, Chomyn A (1995) Complementation and segregation behavior of disease causing mitochondrial DNA mutations in cellular model systems. Biochim Biophys Acta 1271:241–248

Birky CW Jr (1994) Relaxed and stringent genomes: why cytoplasmic genes don't obey Mendel's laws. J Hered 85: 355–365

Boulet L, Karpati G, Shoubridge EA (1992) Distribution and threshold expression of the tRNA(Lys) mutation in skeletal muscle of patients with myoclonic epilepsy and ragged-red fibers (MERRF). Am J Hum Genet 51:1187–1200

Brierley EJ, Johnson MA, Lightowlers RN, James OFW, Turnbull DM (1998) Role of mitochondrial DNA mutations in human aging: implications for the central nervous system and muscle. Ann Neurol 43:217–223

Chinnery PF, Turnbull DM (1997) The clinical features, investigation and management of patients with mitochondrial DNA defects. J Neurol Neurosurg Psychiatry 63:559–563

Clayton DA (1996) Mitochondrial DNA gets the drift. Nat Genet 14:123–125

Flory PJ, Vinograd J (1973) 5-Bromodeoxyuridine labeling of monomeric and catenated circular mitochondrial DNA in HeLa cells. J Mol Biol 74:81–94

Gross NJ, Getz GS, Rabinowitz M (1969) Apparent turnover of mitochondrial deoxyribonucleic acid and mitochondrial phospholipids in the tissues of the rat. J Biol Chem 244: 1552–1562

Hayashi J, Ohta S, Kikuchi A, Takemitsu M, Goto Y, Nonaka I (1991) Introduction of disease-related mitochondrial DNA deletions into HeLa cells lacking mitochondrial DNA results in mitochondrial dysfunction. Proc Natl Acad Sci USA 88: 10614–10618

Howell N (1997) mtDNA recombination: what do in vitro data mean? Am J Hum Genet 61:19–22

Johns D (1995) Mitochondrial DNA and disease. New Engl J Med 333:638–644

Johnson N, Kotz S, Balakrishnan N (1995) Continuous univariate distributions. John Wiley, New York

Kaufmann P, Koga Y, Shanske S, Hirano M, DiMauro S, King MP, Schon EA (1996) Mitochondrial DNA and RNA processing in MELAS. Ann Neurol 40:172–180

Larsson NG, Clayton DA (1995) Molecular genetic aspects

of human mitochondrial disorders. Annu Rev Genet 29: 151–178

Larsson NG, Holme E, Kristiansson B, Oldfors A, Tulinius M (1990) Progressive increase of the mutated mitochondrial DNA fraction in Kearns-Sayre syndrome. Pediatr Res 28: 131–136

Larsson NG, Wang J, Wilhelmsson H, Oldfors A, Rustin P, Lewandoski M, Barsh GS, et al (1998) Mitochondrial transcription factor A is necessary for mtDNA maintenance and embryogenesis in mice. Nat Genet 18:231–236

Lightowlers RN, Chinnery PF, Turnbull DM, Howell N (1997) Mammalian mitochondrial genetics: heredity, heteroplasmy and disease. Trends Genet 13:450–455

Mita S, Schmidt B, Schon EA, DiMauro S, Bonilla E (1989) Detection of "deleted" mitochondrial genomes in cytochrome-c oxidase–deficient fibers of a patient with Kearns-Sayre syndrome. Proc Natl Acad Sci USA 86:9509–9513

Moraes CT, Ricci E, Petruzzella V, Shanske S, DiMauro S, Schon EA, Bonilla E (1992) Molecular analysis of the muscle pathology associated with mitochondrial DNA deletions. Nat Genet 1:359–367

Poulton J, Morten K (1993) Noninvasive diagnosis of the MELAS syndrome from blood DNA. Ann Neurol 34:116

Schon EA, Bonilla E, DiMauro S (1997) Mitochondrial DNA mutations and pathogenesis. J Bioenerg Biomembr 29: 131–149

Shoffner JM (1996) Maternal inheritance and the evaluation of oxidative phosphorylation diseases. Lancet 348: 1283–1288

Shoubridge EA (1994) Mitochondrial DNA diseases: histological and cellular studies. J Bioenerg Biomembr 26: 301–310

Shoubridge EA, Karpati G, Hastings KE (1990) Deletion mutants are functionally dominant over wild-type mitochondrial genomes in skeletal muscle fiber segments in mitochondrial disease. Cell 62:43–49

Tokunaga M, Mita S, Murakami T, Kumamoto T, Uchino M, Nonaka I, Ando M (1994) Single muscle fiber analysis of mitochondrial myopathy, encephalopathy, lactic acidosis, and stroke-like episodes (MELAS). Ann Neurol 35:413–419

Turnbull DM, Lightowlers RN (1998) An essential guide to mtDNA maintenance. Nat Genet 18:199–200

Wallace DC (1992) Diseases of the mitochondrial DNA. Annu Rev Biochem 61:1175–1212

——— (1995) Mitochondrial DNA variation in human evolution, degenerative disease, and aging. Am J Hum Genet 57:201–223

Wallace DC, Shoffner JM, Trounce I, Brown MD, Ballinger SW, Corral-Debrinski M, Horton T, et al (1995) Mitochondrial DNA mutations in human degenerative diseases and aging. Biochim Biophys Acta 1271:141–151

Weber K, Wilson JN, Taylor L, Brierley E, Johnson MA, Turnbull DM, Bindoff LA (1997) A new mtDNA mutation showing accumulation with time and restriction to skeletal muscle. Am J Hum Genet 60:373–380

Zhang H, Cooney DA, Sreenath A, Zhan Q, Agbaria R, Stowe EE, Fornace AJ, et al (1994) Quantitation of mitochondrial DNA in human lymphoblasts by a competitive polymerase chain reaction method: application to the study of inhibitors of mitochondrial DNA content. Mol Pharmacol 46: 1063–1069